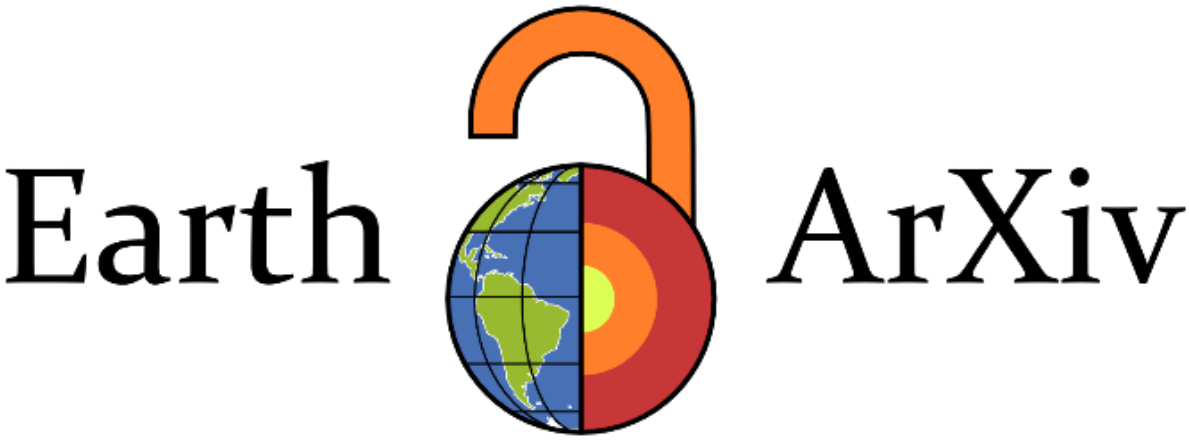

Submitted to: *Environ. Res. Lett.*

Amplified agricultural impacts from more frequent and intense sequential heat events

Raed Hamed[1*], Carmen B. Steinmann[2,3*], Qiyun Ma[4], Daniel Balanzategui[5,6,7], Ellie Broadman[8], Corey Lesk[9] and Kai Kornhuber[10,11]

[1]Institute for Environmental Studies (IVM), Vrije Universiteit Amsterdam, Amsterdam, 1081, the Netherlands.
[2]Institute for Environmental Decisions, ETH Zurich, Zurich, 8092, Switzerland.
[3] Federal Office of Meteorology and Climatology MeteoSwiss, Zurich, 8058, Switzerland
[4] Alfred Wegener Institute, Helmholtz Centre for Polar and Marine Research, Bremerhaven, 27570, Germany.
[5] Materials Testing Institute, University of Applied Sciences, Luebeck, 23562, Germany.
[6] Department of Natural Sciences, German Archaeology Institute DAI, Berlin, 14195, Germany.
[7] Geography Department, Humboldt University of Berlin, Berlin, 10117, Germany.
[8] Laboratory of Tree-Ring Research, University of Arizona, Tucson, 85721, USA.
[9] Department of Geography, Neukom Institute for Computational Science, Dartmouth College, Hanover, 03755, USA.
[10] Lamont-Doherty Earth Observatory, Columbia University, Palisades, 10964, USA.
[11] International Institute for Applied Systems Analysis, Laxenburg, 2361, Austria.
[*]These authors contributed equally to this work.

E-mail: carmen.steinmann@usys.ethz.ch

Keywords: Compound Events, Food Production, Heat Extremes, Climate Change

Abstract. As the climate warms, interacting weather extremes such as sequential heat events pose complex risks to societies. Regarding global agriculture, laboratory experiments suggest that early crop exposure to heat may either confer tolerance or enhance vulnerability to subsequent heat during the critical crop flowering stage. We show that warm early-seasons improve crop yield potential, particularly for soybean and maize, but also increase the impacts of subsequent heat by 5% to 55% compared to years with average early-season temperatures. The impacts of this increased yield sensitivity outweigh the benefits of early season heat when mid-season temperature anomalies exceed 0.7-5 °C (depending on the crop). Analyzing projected temperatures under the Shared Socioeconomic Pathway 3-7.0, we find a tenfold increase in the likelihood of experiencing sequential heat in early and mid-season crop growth stages, defined as a joint 90$^{\text{th}}$ percentile event. Accounting for the interactive effects of early and mid-season warming increases projected temperature-related crop yield losses by 2–44%, depending on crop and region. These results underline the emerging nonlinear risks from sequential heat extremes to food systems, which can largely be avoided when limiting warming to 1.5 °C globally.

1. Introduction

Climate and weather extremes often have detrimental effects on crop production (Lesk et al.; 2016; Vogel et al.; 2021), especially when multiple extremes occur within the same growing season (Zscheischler et al.; 2018). While the compounding impacts of combined heat and drought on crops have drawn substantial attention (Hamed et al.; 2021; Lesk et al.; 2021), the occurrence of more complex combinations of weather and climate extremes is becoming increasingly likely as the climate warms. Sequential (in other words, consecutive or temporally compounding) heat extremes are a particularly salient example, as they are projected to become more likely and reach greater intensities as growing seasons get warmer and begin earlier (Raymond et al.; 2022; Baldwin et al.; 2019).

The likelihood of sequential heat extremes is expected to increase as individual seasons warm due to the thermodynamic response to rising greenhouse gas concentrations (Robinson et al.; 2021). Additionally, more complex climate change effects involve potential changes in the dependence between seasonal heat (Weiland et al.; 2021). For example, warmer springs will likely feature lower soil moisture due to the direct drying effect of spring heat combined with the indirect effects of earlier snowmelt and vegetation green-up. A drier land surface during spring can prime the surface energy balance and boundary layer in ways that enhance the causal connection between sequential heat events, increasing their likelihood by more than what would be expected from warming alone (Gloege et al.; 2022).

While thermal limitations in crop species are well studied, little is known about the impact of sequential hot seasons on crops at the scale of regional production. In small-scale experiments, early crop exposure to heat stress triggers myriad physiological responses with lasting effects on vegetative growth, yield processes, and stress signaling and response pathways (Hossain et al.; 2018; Antoniou et al.; 2016; Mittler et al.; 2012). Competing responses to early heat exposure can confer tolerance (acclimation) or worsen susceptibility (accumulating or compounding stress) to subsequent heat (WANG et al.; 2017; Liu et al.; 2022; Nadeem et al.; 2018), and may be dependent on region and crop type. As a result, it is unclear whether the cumulative effect of these inter-seasonal heat responses helps or hinders crops confronted by consecutive heat stress.

Here, we clarify the impact of sequential warm seasons on yields for staple crops at local and regional production scales across the United States (US) and Europe (EU) over the past four decades. We introduce a statistical model that isolates the interactive effect of sequential heat on observed maize, soybean, barley, and wheat yields. We then investigate future frequency changes in sequential heat using Coupled Model Intercomparison Project 6 (CMIP6) model experiments under different emission scenarios. Finally, we compute the associated expected future crop yield losses, including impacts from compounding sequential heat events. We conclude by highlighting the urgent need to consider enhanced non-linear impacts to crops resulting from the increased intensity and likelihood of sequential heat events. This is essential for a more

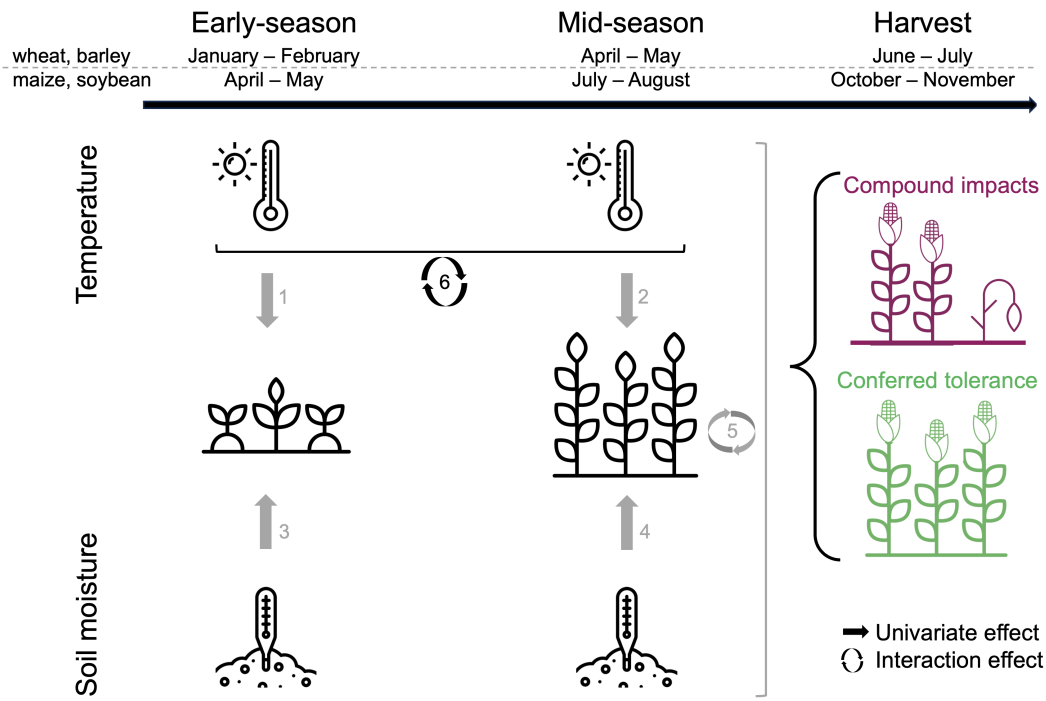

Figure 1. Impacts of compound temperature and soil moisture extremes on crop yields. Straight arrows represent univariate effects of temperature (1 early-season, 2 mid-season) and soil moisture (3 early-season, 4 mid-season). Circular arrows represent the interactive effects of mid-season co-occurring interactive effects of temperature and soil moisture and sequential early and late seasonal temperature anomalies (arrow 6). The interactive effect of sequential early- and mid-season temperature (arrow 6) is the core focus of this study, while we control for the effects represented by the remaining gray arrows.

accurate estimation of future risks to the food system, facilitating the adaptation of cropping systems to increasingly sequential extremes.

2. Data and Methods

2.1. A statistical model to attribute yield losses to univariate and compound weather conditions across seasons

We use crop- and region-specific mixed-effects models to relate crop yield $Y_t^{(c)}$ in county c and year t (1980–2020) to seasonal climate anomalies and temporal trends. The fixed effects include linear and quadratic terms for mean maximum temperature (T) and soil moisture (M) during early (e) and mid-season (m) growth stages, along with interaction terms for sequential temperature effects and compound heat-moisture stress. A linear time trend t captures gradual changes from climate and technological progress. To account for spatial heterogeneity, we include county-level random intercepts $u_0^{(c)}$ and random slopes $u_1^{(c)}t$. The full model is specified as:

$$
\begin{aligned}
Y_t^{(c)} = \beta_0 &+ \beta_1 T_{e,t}^{(c)} + \beta_2 T_{m,t}^{(c)} + \beta_3 \left(T_{e,t}^{(c)}\right)^2 \\
&+ \beta_4 \left(T_{m,t}^{(c)}\right)^2 + \beta_5 M_{e,t}^{(c)} + \beta_6 M_{m,t}^{(c)} \\
&+ \beta_7 \left(M_{e,t}^{(c)}\right)^2 + \beta_8 \left(M_{m,t}^{(c)}\right)^2 \\
&+ \beta_9 \left(T_{e,t}^{(c)} T_{m,t}^{(c)}\right) + \beta_{10} \left(T_{m,t}^{(c)} M_{m,t}^{(c)}\right) \\
&+ \beta_{11} t + u_0^{(c)} + u_1^{(c)} t + \varepsilon_t^{(c)}
\end{aligned} \tag{1}
$$

We weight each observation by harvested area so that high-production counties exert proportionally greater influence on fixed-effect estimates. To ensure agronomic comparability, we include only counties where cropping calendars align with the following criteria: soybean and maize are planted in April–May and wheat and barley reach maturity in June–July. Accordingly, we define the early and mid-seasons as April–May and July–August for soybean and maize, and January–February and April-May for wheat and barley. We further limit the sample to counties that are at least 90% rain-fed to avoid confounding effects from irrigation (Fig. S8), and require a minimum of 25 years of yield and weather data per county to enable robust statistical inference. Crop calendars and irrigation status are derived from the MIRCA-OS dataset (Kebede et al.; 2025).

2.2. Historic crop and climate data.

County-level yield (metric tons per hectare, t/ha) and harvested area (hectares, ha) data for soy, maize, and wheat in the US from 1980 to 2020 are obtained from the USDA dataset `https://quickstats.nass.usda.gov/`, last access: 15 November 2022). Sub-regional yield (t/ha) and harvested area (ha) for soft wheat, winter barley and maize in the EU from 1980 to 2020 are sourced from the EUROSTAT dataset (`https://ec.europa.eu/eurostat/web/agriculture/`, last access: 1 May 2024). Harvested area is utilized as weights both in fitting the model and for spatial averaging across crop regions.

Root zone soil moisture and maximum temperature variables are obtained from GLEAM v3.5a (Martens et al.; 2017) and CPC datasets (CPC Global Unified Temperature data provided by the NOAA PSL, Boulder, Colorado, USA, from their website at `https://psl.noaa.gov`), respectively. GLEAM is a model-based dataset forced with satellite and reanalysis data, while CPC leverages station-based observations. We filter these datasets for the study period and average them over two-month intervals to represent early and mid-season weather conditions. These intervals roughly align with the dominant regional vegetative and flowering crop stages identified in the Crop Calendar Dataset (Sacks et al.; 2010). Soil moisture is standardized at the county level to reflect local drought conditions, similar to the SPEI approach (Stagge et al.; 2015). All climate variables are spatially averaged to correspond to sub-regional crop yield administrative units.

2.3. Projecting changes in the frequency of sequential heat extremes.

To analyse changes in frequency of sequential heat extremes, we make use of CMIP6 projections for four different emission scenarios: SSP1-1.9 (9 models) and SSP1-2.6 (22 models), SSP2-4.5 (15 models), SSP3-7.0 (15 models). The choice of models per scenario are described in Table S3.

We set the 90th percentile of the joint early and mid-season temperature ranks during the historic period as our baseline to define sequential extreme heat events (i.e., the warmest 10% of sequential heat years). For each year i, the count threshold is computed as

$$C_i = \sum_{j=1}^{n} \mathbf{1}\{T_{\text{early},i} \geq T_{\text{early},j} \text{ and } T_{\text{mid},i} \geq T_{\text{mid},j}\} \tag{2}$$

where $\mathbf{1}\{\cdot\}$ is the indicator function that equals 1 if the condition holds and 0 otherwise, and n is the total number of years in the dataset. A year is classified as extreme if its C_i exceeds the historical 90th percentile.

We then compute the frequency of extreme events for each combination of ssp scenario, model, and crop pair and derive a likelihood multiplication factor by comparing these frequencies to the historic baseline.

In addition, we calculate count thresholds C_i independently for each period and assess changes in the relative frequency of extreme events compared to the historic period. This complementary approach provides insights into potential shifts in the tail behavior and dependence structure between early and mid-season temperatures.

2.4. Projecting compound crop impacts from sequential spring and summer warming.

We calculate 40-year yield estimates for both a historical period (1975–2015) and a future period (2060–2100) using each CMIP6 model. This forms the basis to analyze changes in mean yields, which are weighted by harvested area as per period (2010-2020).

We first compute changes in average maximum temperature $\overline{\Delta T_s^c}$ for each season s (early (e) and mid (m)) and county c between the historic (1975-2015) and future (2060-2100) 40-year periods for each CMIP6 model. Second, we combine these delta changes with the historical estimated model coefficients (see Section 2.1) to project future yield changes ($\overline{\Delta Y^c}$, Eq. 3) – function of early-season, mid-season and interactive temperature effects.

$$\overline{\Delta Y} = \beta_1\,\overline{\Delta T_e} + \beta_3\,\overline{\Delta T_e^2} + \beta_2\,\overline{\Delta T_m} + \beta_4\,\overline{\Delta T_m^2} + \beta_9\,\overline{\Delta T_e\,\Delta T_m}. \tag{3}$$

3. Results

3.1. Negative effects of sequential hot conditions on crop yields

Our prime objective in this study is to quantify the effects of sequential heat on crop yields. In particular, we are interested in the interactive effect of early and mid-season

temperature conditions beyond the impacts of each separately. For this, we develop crop- and region-specific mixed-effects models linking crop yields to mean maximum temperature and soil moisture anomalies during early and mid-season crop growth stages (see Methods). For soybean and maize, the early season is April–May and the mid-season July–August; for wheat and barley, the early season is January–February and the mid-season April-May (see Methods). Non-linear responses are captured with linear and quadratic terms for each variable in both seasons. Interaction terms between mid-season temperature and soil moisture represent well-documented impacts of compound hot and dry conditions on crop yields (Lesk et al.; 2022), while interactions between early- and mid-season temperature test for sequential heat effects.

Explicitly including soil moisture is in line with recent efforts aimed at better disentangling water and heat stress in statistical models (Proctor et al.; 2022; Rigden et al.; 2020). Separating moisture and heat stress is important as their impacts reflect distinct physiological mechanisms and therefore would eventually require different adaptation strategies (Suzuki et al.; 2014). Figure 1 illustrates the fitted relationships; full coefficient estimates appear in Table S1 and Table S2. Our statistical model explains roughly half of the variability in soybean and maize yields (soybean-US:59%, maize-US:66%, maize-EU: 42%) and 24% of barley in the EU. The predictability for wheat in both the US and the EU is considerably lower (wheat-US: 17%, wheat-EU: 5%).

Our statistical model detects yield effects of temperature and soil moisture within the early-season and mid-season periods. Warm early-season temperatures generally enhance yield potential, but for wheat and barley, above-average early-season warmth reduces yields (Fig. S1). Wet early-season conditions lower yields for soybean, maize, and barley, but benefit wheat in both the EU and US (Fig. S2). In the mid-season, heat consistently reduces yields across all crops (Fig. S3). Wet conditions generally boost yields, except for wheat and barley in the EU, where excess moisture leads to losses. Notably, extreme wet conditions negatively affect all crops (Fig. S4). We also find that co-occurring hot and dry conditions produce synergistic impacts that significantly amplify yield losses for all crops beyond the simple additive effects of temperature and soil moisture anomalies (Fig. S5). The varying sensitivities of crops to early- and mid-season temperature and moisture conditions are consistent with results highlighted in previous work (Ortiz-Bobea et al.; 2019; Butler and Huybers; 2015), along with the compounding effects of hot and dry conditions (Hamed et al.; 2021; Lesk et al.; 2021).

However, we also find an additional compounding impact from interactions between early- and mid-season temperatures (Fig. 1, arrow 6). These interactions are negative for all crops and regions, though they are less pronounced for wheat. This suggests that crop yield sensitivity to mid-season temperature depends on the temperature experienced during the early season. Specifically, while high early-season temperatures are generally beneficial, they appear to prime crops for stronger negative responses to heat later in the season. These effects are not captured by early- or mid-season temperature alone and emerge despite controlling for soil moisture and compound heat–moisture interactions.

The important effect of early-season heat in pre-conditioning crop yield responses

to subsequent mid-season heat is confirmed by both yield and climate observations (bins, Fig. 2), and by our statistical models (contours, Fig. 2) for crops both in the US and EU. Yields exhibit non-linear bivariate dependence structures with respect to early- and mid-season temperatures. We express yield changes relative to the trend-based expected yield. Notably, the strongest negative yield anomalies occur when hot mid-seasons follow warmer-than-average early-seasons (upper right quadrants, Fig. 2). In such growing seasons, yield losses are approximately four times larger compared to hot mid-seasons following an early season with average to below-average temperatures (bottom right quadrant, Fig. 2A, B). While years with warm springs are more likely to be dry, the statistical results in Fig. 2 isolate the interactive effect of inter-seasonal temperature using controls on early- and mid-season soil moisture. This result thus highlights sequential early- and mid-season heat as a notable climate risk to crop yields over recent decades.

The nonlinear relationship between crop yields and temperature anomalies reveals that sensitivity to mid-season heat is modulated by early-season temperatures. To illustrate this, we show yield responses to mid-season temperatures under the 5^{th} (cold), 50^{th} (normal), and 95^{th} (hot) percentiles of early-season temperature (Fig. 3). Yields decline more steeply with rising mid-season temperatures following a hot early-season compared to normal early conditions (red vs. grey lines, Fig. 3). This increased sensitivity varies by crop and region: soybean shows a 36% higher sensitivity, maize 25% (US) and 16% (EU), and barley the most at 56%. In contrast, wheat shows only a marginal increase (5%) in both regions. The differences roughly double when comparing cold versus hot early-season preconditions (blue vs. red lines, Fig. 3). While mid-season heat has long been recognized as a key driver of yield loss, these results show that its impact is amplified by preceding early-season warmth.

Yield benefits from warm early-seasons (red vs. blue lines, Fig. 3) only materialize under cool-to-normal mid-season conditions and are largely canceled out when followed by hot mid-seasons. We identify crop-specific mid-season temperature thresholds beyond which early-season warmth results in net yield losses: 5 °C for US maize, 3.6 °C for US soybean, 3.5 °C for EU maize, and just 0.7 °C for EU barley (vertical red dashed line, Fig.3). Beyond these thresholds, early-season warmth amplifies mid-season heat sensitivity enough to negate the yield benefits of early-season heat. This pattern reflects an interactive effect, where early-season conditions alter mid-season yield responses, rather than a simple additive effect of temperature across the two periods. In contrast, wheat shows neither benefits from warm early-seasons nor a clear modulation of mid-season sensitivity (Fig. 3D, E).

3.2. Amplified risks of sequential heat events beyond +1.5 °C of global warming

Prior projections of crop yields under climate change generally conclude that yield losses from warmer mid-seasons outstrip the benefits of early-season warming, except in the coldest cropping regions (Ortiz-Bobea et al.; 2019; Ray et al.; 2019; Butler and Huybers;

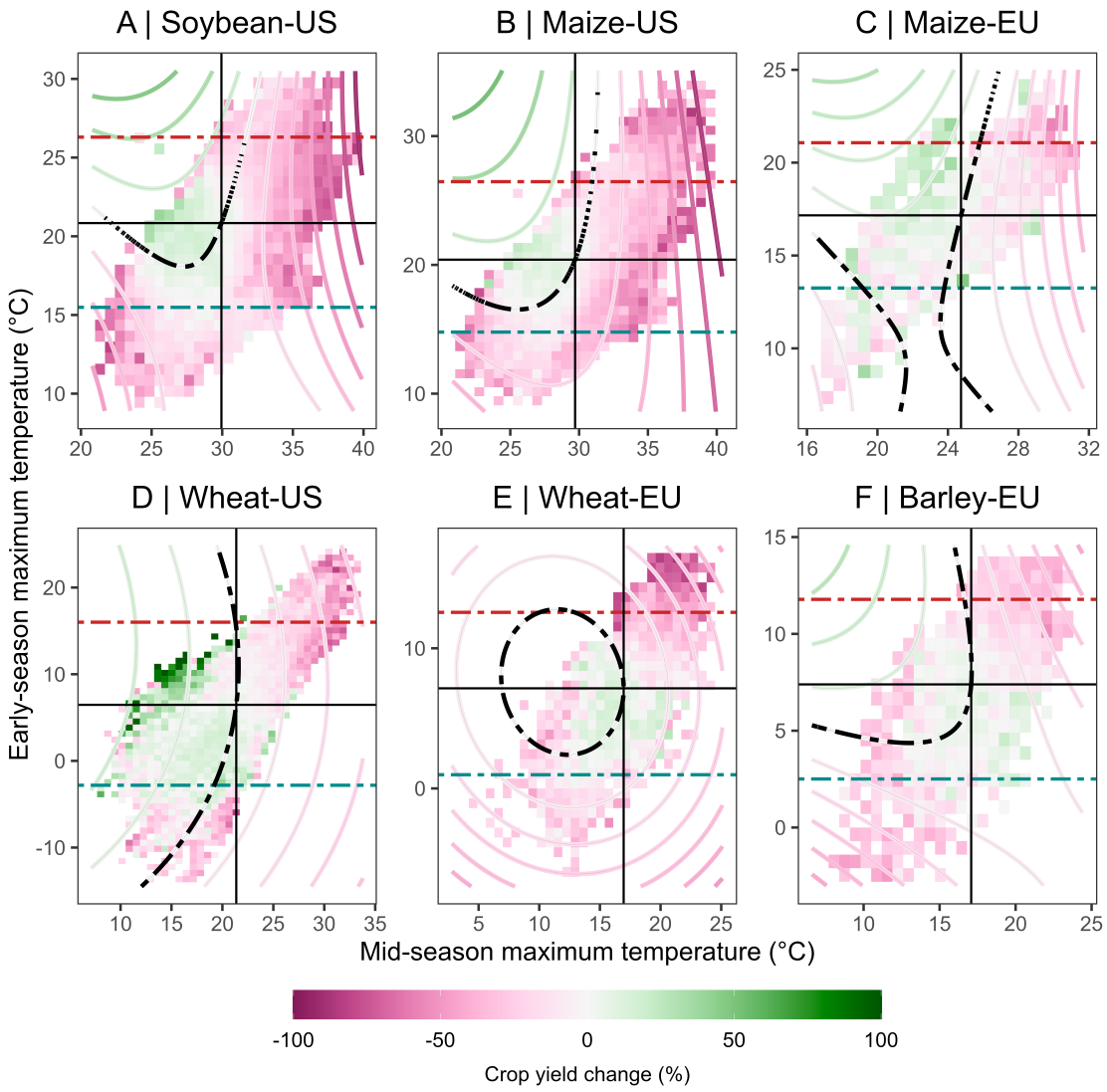

Figure 2. Yield sensitivity to early and mid-season mean maximum temperature. Observed yield anomalies relative to the trend-based expected yield are stratified by different early- and mid-season temperature levels (shaded bins; bin size = 0.7°C). Contour lines represent yield anomalies based on the statistical model. The dotted black curve shows joint early and mid-season conditions conducive to average yield estimates. Dotted blue and red lines represent the 5^{th} and 95^{th} percentiles of early-season temperature conditions. Solid black lines indicate the average early- and mid-season temperature conditions.

2015). However, our findings suggest that this balance may further depend on the conditioned influence of early-season temperatures on crop responses to subsequent mid-season heat. This insight implies that future yield projections depend on the relative seasonal rates of warming and concurrence of early- and mid-season heat anomalies. To assess future risks of sequential heat events, we use climate projections from CMIP6 model experiments (see Table S3) under emission scenarios compatible with the 1.5

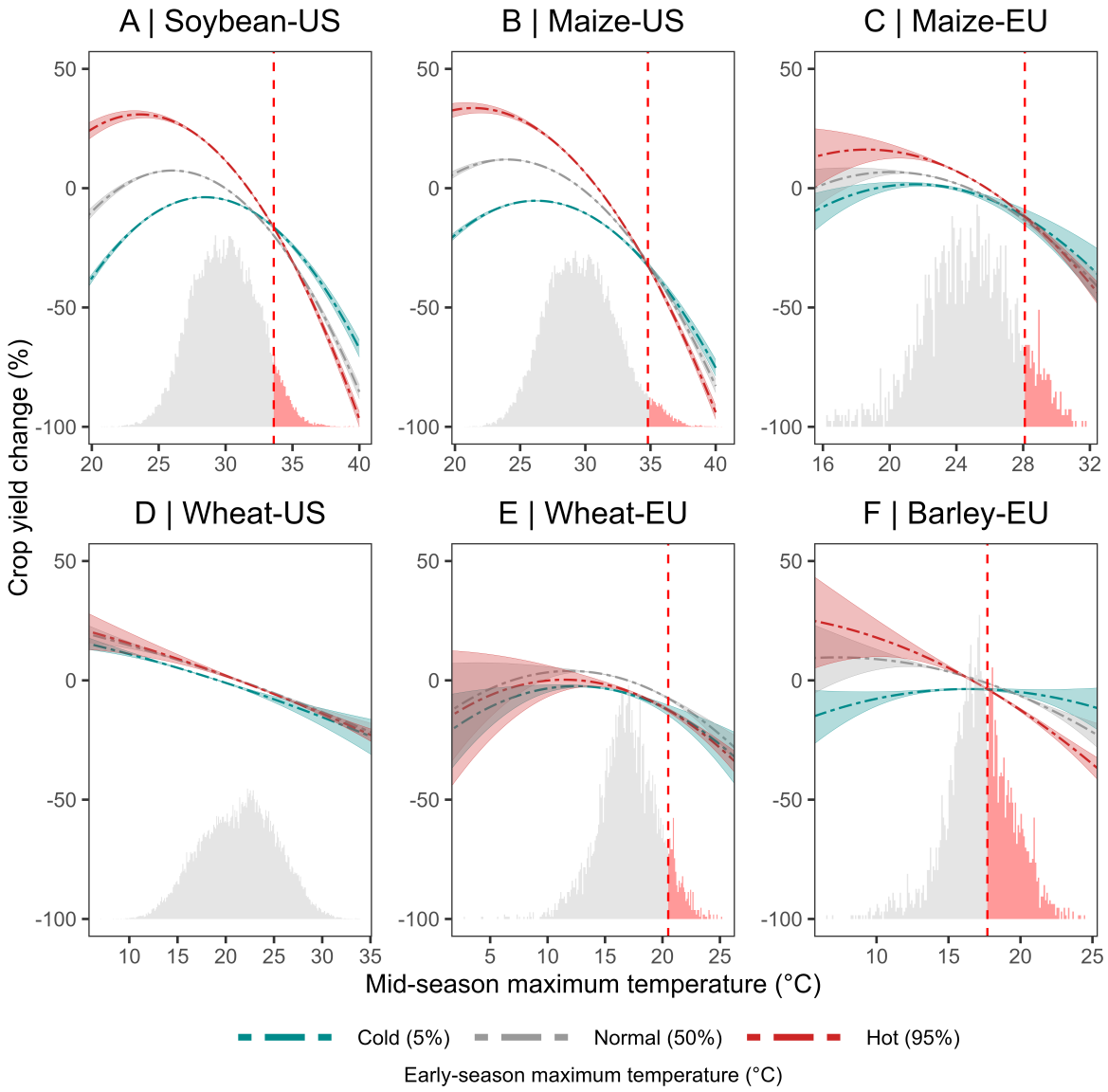

Figure 3. Modeled dependence of yield sensitivity to mid-season temperatures on early-season temperature percentile. The Y-axis shows yield anomalies relative to the trend-based expected yield, as a function of mid-season temperature levels. These sensitivities are shown separately for three different early-season temperature percentiles (5^{th} in blue, 50^{th} in grey, and 95^{th} in red). Shading represents the associated 95% confidence intervals for the estimated effects. Histograms display the distribution of mid-season maximum temperatures.

degree guardrail stated in the Paris Agreement (mitigation scenarios SSP1-1.9 and SSP1-2.6), the current-policy scenario (SSP2-4.5), and a high-emissions scenario (SSP3-7.0). Note that the number of models differs between SSP scenarios (see Table S3), but that we do provide results also for the 8 climate models shared across scenarios (Fig. S6).

Temperature increases become more pronounced under higher emission scenarios. Under SSP2-4.5, we project additional warming of 2.7 °C in the early season and 3.5 °C

in the mid-season over soybean and maize growing areas in the US by the end of the century. For wheat, the increase is 2.9 °C and 2.8 °C, respectively, compared to historical conditions from 1975 to 2015. In the EU, maize is projected to experience 2.2 °C of early-season and 3.9 °C of mid-season warming, while wheat and barley show smaller increases of 2 °C in both growth stage periods (Fig. S7). These differences between crops within the same region are mainly due to variations in the timing of early- and mid-season growth stages. That is, early-season conditions for wheat and barley occur in February and March, whereas for soybean and maize, they fall in April and May.

The frequency of sequential heat extremes, defined as the 10 percent most extreme combinations of early- and mid-season heat during the historical period (see Data and Methods), increases substantially with emissions. We find that sequential heat extremes are 10 times more likely under a high-emission scenario (SSP3-7.0), 8 times more likely under SSP2-4.5, and 5 times more likely even under stringent mitigation (SSP1-1.9) (Fig. 4).

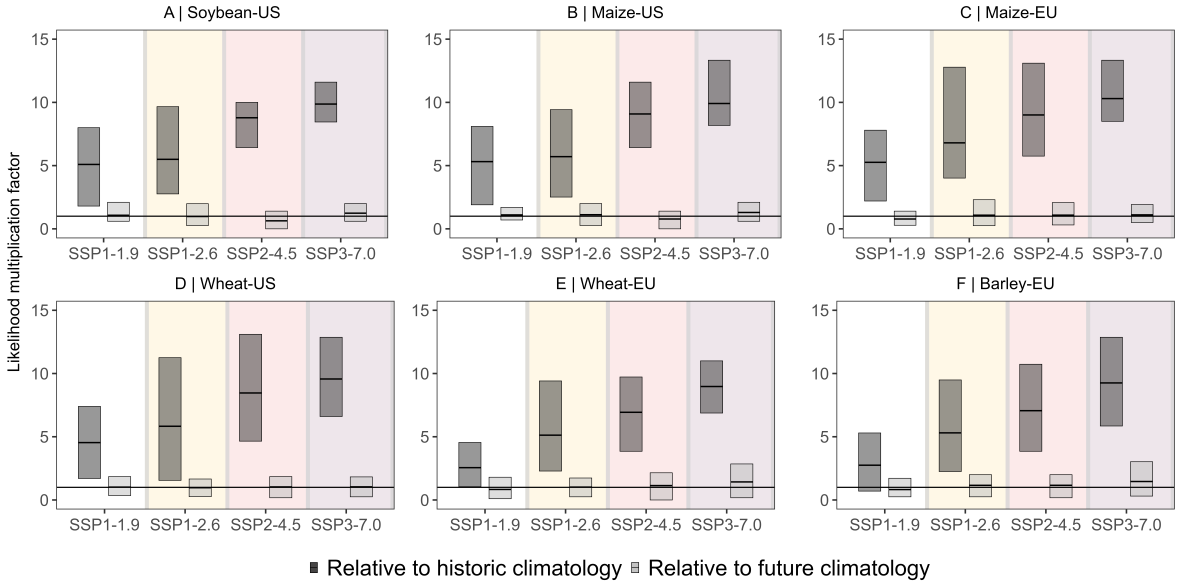

Figure 4. Projected frequency changes in sequential heat events for the time period 2060–2100 under different emission scenarios: SSP1-1.9 (number models n=9), SSP1-2.6 (n=22), SSP2-4.5 (n=15), SSP3-7.0(n=15). The change in event frequency represents a weighted spatial average over harvesting regions and is defined as the frequency of events exceeding the 90^{th} percentile of joint early- and mid-season temperature extremes for two cases: 1)frequency change relative to historic climatology (1975–2015), 2)frequency change relative to future climatology (2060–2100). Bars show average climate model projections, while error bars show the spread across models.

To account for changes in the climate baseline, we also examine frequency shifts using a relative definition of sequential heat extremes that adjusts to future climatological conditions (Fig. 4). This approach allows us to detect changes in the dependence between early- and mid-season heat, beyond expected increases in

absolute temperatures. Under this definition, relative event frequency remains largely unchanged across emission scenarios. However, models show persistent disagreement on the direction of change, indicating high uncertainty in projections of relative sequential heat risk. This uncertainty is likely linked to uncertainties in land–atmosphere feedback or circulation changes under forcing (Shepherd; 2014; Sippel et al.; 2017; Dong et al.; 2022).

3.3. Enhanced impacts on yield production from increasingly sequential heat events under future emission scenarios

To evaluate crop risks from projected warming in the context of interactive seasonal temperature effects, we apply our crop-climate models using early- and mid-season temperature projections. Under SSP2-4.5, soybean and maize yields decline by 13–19% on average (up to 35% in some models), while wheat and barley losses are smaller (around 4–5%), with consistent sign agreement across all CMIP6 models (Fig. 5). These results suggest that crop type, rather than region, is the dominant factor shaping total yield sensitivity to warming.

However, the yield impacts of early- and mid-season temperature anomalies, and their interaction, varies across crops and regions. Early-season warming benefits soybean and maize, especially in the US, but has little effect on wheat and barley in either the US and EU (Fig. 5). Joint warming of early and mid-seasons substantially amplifies yield losses for maize, soybean, and barley (Fig. 5A-C, F), but has minimal impact on wheat (Fig. 5D, E). In many cases, the losses from this inter-seasonal interaction effect cancel out or even exceed the gains from warmer early seasons under the SSP2-4.5 scenario and beyond. Ignoring this interaction under SSP3-7.0 leads to underestimated losses of 2–3% for wheat (EU, US), 19–22% for maize (EU, US), 33% for US soybean, and 44% for EU barley (Fig. 5, comparing total including and excluding the contribution of the temperature interaction). This highlights the importance of accounting for the inter-seasonal dependence of yield sensitivities to heat in future crop-climate risk assessments.

Importantly, our results show that nonlinear yield losses from sequential heat can be substantially mitigated by limiting global warming to 1.5 °C (SSP1-1.9), where projected losses are restricted to 1–6% compared to expected yield, albeit with significant model uncertainty (Fig. 5).

Discussion & Conclusion

Sequential heat extremes are a growing climate risk with potentially non-linear impacts on natural and societal systems. In this study, we assess the sensitivity of several crop types to sequential temperature and soil moisture anomalies using a statistical framework. Relying on observations avoids the key limitations of current process-based crop models, which struggle to capture extreme heat impacts and do not explicitly simulate interactions between key stress stimuli (Heinicke et al.; 2022; Schewe et al.; 2019; Asseng

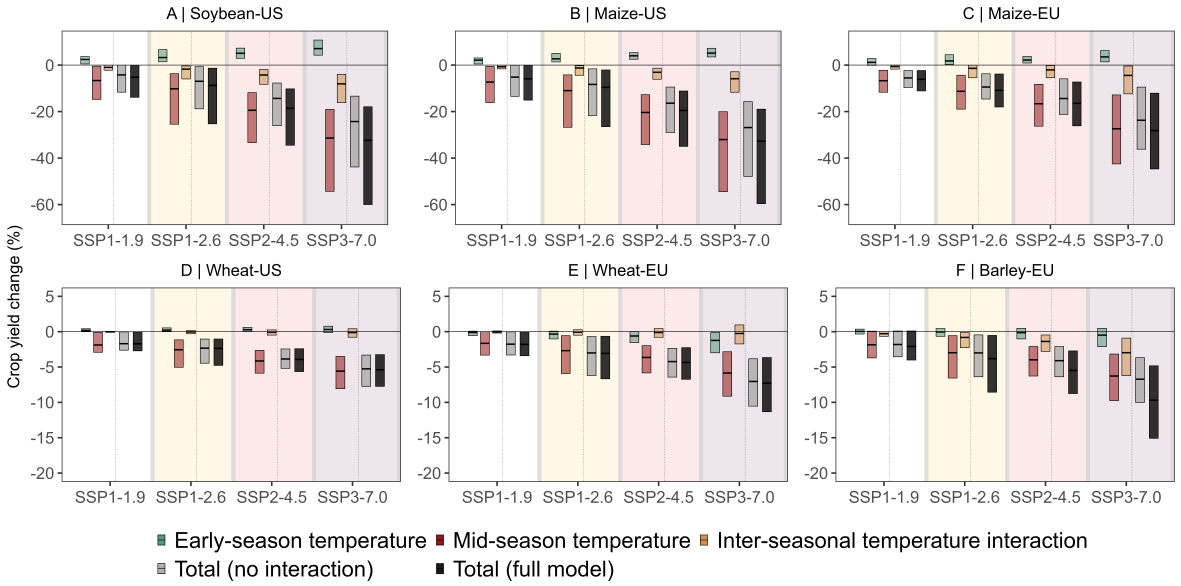

Figure 5. Projected crop production changes for the future period (2060–2100) compared to historic (1975–2015) under different emission scenarios: SSP1-1.9 (number models n=9), SSP1-2.6 (n=22), SSP2-4.5 (n=15), SSP3-7.0(n=15). Average crop yield losses are attributed to early- and mid-season temperature changes and their interaction. Bar show average projected losses, while error bars show the 5–95% range accounting for regression and model projection uncertainties.

et al.; 2015; Nóia Júnior et al.; 2025), leading to an underestimation of projected yield losses (Kornhuber et al.; 2023). Although our model does not capture the full range of agronomic factors affecting yield, the inclusion of terms t and u allows us to account for some of these influences (Equation 1). Specifically, the t term reflects long-term trends in yield, which is extensively used as a proxy for technological advancements, adoption of new cultivars, and the CO_2 fertilization effect during the study period (Liu et al.; 2016). The u term captures systematic, time-invariant differences between counties, including baseline management practices and soil quality. However, in future projections, we only study the effects on yields driven by sequential heat events, assuming changes in agronomic factors, and sensitivities to environmental conditions remain at their observed historical levels. This ignores potential adaptation measures that could contribute significantly to future yields (Aggarwal et al.; 2019).

Within the climate system, both spring warmth (Gloege et al.; 2022) and the interrelationship between temperature and soil moisture (Miralles et al.; 2014) can drive heat extremes during summertime. Here, we control for soil moisture and its interaction with mid-season temperature. Additionally, we control for a potential direct, non-linear heat response in both seasons separately by including quadratic temperature terms. This approach pinpoints the influence of early-season heat exposure on crop responses during the mid-season, independent of both the potential physical coupling between temperature in both seasons and the non-linear impacts of soil moisture and its interplay with

temperature on crop yields. We focus on temperature and soil moisture across seasons as principal drivers of crop yields (Butler and Huybers; 2015; Ortiz-Bobea et al.; 2019) and disregard other correlated climatic factors such as radiation, wind, humidity, and CO_2, which also play distinct, but secondary roles. Future research can further disentangle these drivers for more detailed process attribution and improved representation in yield projections.

We find amplified yield losses from mid-season heat preceded by warm early seasons. This interaction is consistent across crops and regions, though weaker for wheat. The results reveal an underappreciated climate risk to crops beyond 1.5 °C warming, with important implications for compound stress assessments and adaptation planning. In field and laboratory experiments, certain crop responses to early heat exposure have been shown to confer acquired thermotolerance (or 'heat priming'). Key physiological tolerances such as cell membrane stability and water-use efficiency at high temperatures can be enhanced when young crops experience heat (WANG et al.; 2017; Liu et al.; 2022; Nadeem et al.; 2018). However, our results suggest that at regional crop-production scales, these yield-benefiting responses are outweighed by compounding stress interactions (Hossain et al.; 2018; Antoniou et al.; 2016; Mittler et al.; 2012). For instance, the accumulation of reactive oxygen species due to early-season heat may raise baseline plant stress, and thus heat sensitivity, during the flowering stage (Choudhury et al.; 2017). Moreover, warm early conditions may also promote pathogen development, increasing crop susceptibility to later-season heat stress (Dixit et al.; 2024).

The structure of interactive heat effects highlights the balance between early-season gains and mid-season heat damage. Warmer early-season conditions increase net yield for all crops except barley and wheat, which show signs of early-season heat stress above average levels, particularly in the EU (Fig. 5D,E). These responses are consistent with prior findings on regional sensitivity (Ben-Ari et al.; 2018) and reported impacts of early heat stress on photosynthesis and tissue development in barley and wheat (Mendanha et al.; 2018; Nadeem et al.; 2018). For soybean and maize, however, yield gains due to warmer early-season temperatures are negated by exacerbated losses from mid-season heat. We interpret these losses as due to enhanced mid-season yield sensitivity to heat, consistent with physiological literature. An alternative explanation is that mid-season heat prevents crops from realizing the benefits of early-season warming such as improved germination rates (Butler et al.; 2014), a potential gain in yield that can only be realized alongside favorable mid-season conditions.

While the overall direction of sequential heat impacts is consistent across regions, the temperature thresholds at which benefits of early heat are completely negated by the increased sensitivity to mid-season heat differ. For example, maize yields decline under sequential heat in both the EU and the US, but the mid-season temperature at which interaction losses outweigh early-season gains is lower in the EU (28 °C) than in the US (35 °C), corresponding to anomalies of 3.6 °C and 5 °C, respectively.

This suggests that although the response direction is consistent, regional differences in cultivar, management, or baseline climate modulate the interactive effects of early- and mid-season heat.

A notable difference is the response of wheat to sequential heat, which is weaker than that of barley, even though both share similar planting and harvesting windows. This contrast may stem from physiological and developmental differences. Experimental evidence shows that both wheat and barley are highly sensitive to heat during reproductive development, particularly around anthesis and grain filling. In addition, both wheat and barley are sensitive to early-season heat, which can delay inflorescence development and reduce spikelet formation (Jacott and Boden; 2020). However, wheat more frequently exhibits accelerated phenology and greater acclimation capacity (Jacott and Boden; 2020), which may enable partial recovery from early-season stress. For example, in Germany, warmer springs have advanced wheat heading by up to 14 days over recent decades, a shift estimated to almost fully offset the warming-induced increase in anthesis heat stress, with potential impacts being 60% greater if phenology did not advance (Rezaei et al.; 2015). Globally, wheat growing seasons have shortened and heading dates have advanced by ∼2 days per decade on average (Ren et al.; 2019; Hu et al.; 2005), highlighting the widespread acceleration of wheat phenology under warming. Barley may lack such phenological flexibility, which is consistent with the stronger sequential heat interaction effects observed for this crop in our analysis. Some of the differences in wheat's sequential heat sensitivity may also reflect differences in model skill between crops. More broadly, our findings suggest that the impacts of sequential heat exposure vary across crops, reflecting underlying genetic and physiological traits (Jagadish et al.; 2021), and may also vary across regions for a given crop due to differences in climate, management, or soils.

Our core conclusion is that increasingly sequential heat events will have non-linear and compounding impacts on crop yields under higher levels of warming. Projected yield losses from sequential heat often offset, and in some cases exceed, the benefits of warmer early-season conditions under high emission scenarios (SSP2-4.5 and SSP3-7.0). This study isolates the effects of sequential heat in a warming climate, rather than providing a full assessment of future climate change impacts. While we control for soil moisture in our models, we do not account for projected changes in moisture availability, which remain highly uncertain compared to temperature projections (Cheng et al.; 2017). However, future soil moisture changes could further amplify losses, both directly and through enhanced heat-drought interactions (Hamed et al.; 2025).

Given the key role of soil moisture in modulating crop yields and surface temperature, future work could integrate scenario-based moisture pathways to explore potential yield outcomes. This would help better characterize both aleatoric and epistemic uncertainty in projections. One example is the 2023 Dutch climate scenarios (KNMI'23), which include wet and dry variants for each emission pathway (Bessembinder et al.; 2023). Such storyline frameworks offer a valuable approach for

improving preparedness under a wide range of plausible futures. Similarly, irrigation can substantially alter crop responses to heat (Troy et al.; 2015) and robustly accounting for future irrigation availability is an important avenue for future research.

To conclude, our analysis underlines the need for anticipating nonlinear crop production impacts from sequential heat, a form of temporally compound extreme that merits further attention. Our results also highlight how reducing emissions can limit these risks within relatively manageable margins. Furthermore, our findings underscore the need to improve our understanding of interacting impact mechanisms, and enhance the resilience of crop varieties and the global food system to effectively adapt to future complex climate risks. For instance, our findings suggest that climate-adaptive crop development may achieve greater yields under warming by selectively breeding not only for mid-season heat tolerance, but for tolerance to combinations of early- and mid-season heat. This approach may help capture potential benefits of warmer early seasons, especially in combination with agronomic developments, such as earlier sowing. Along with mitigation efforts, our results illustrate the importance of bridging the detailed physiological insights arising from small-scale experiments with emerging, production-relevant insights available from regional statistical analyses for effective adaptation planning.

Acknowledgments

This work emerged from the Training School on Statistical Modelling of Compound Events which took place in Como, Italy in September/October 2022. C.B.S received funding from the Swiss Innovation Agency Innosuisse under Grant Agreement No 53733.1 IP-SBM. Q.M. is supported by funding from the Federal Ministry of Education and Research (BMBF) and the Helmholtz Research Field Earth & Environment for the Innovation Pool Project SCENIC. C.L. received funding from FRQNT (31916) and the Dartmouth Neukom Institute for Computational Science. DB was supported by the "Groundcheck" research cluster of the German Archaeological Institute (DAI).

Author contributions

All authors (RH., C.B.S., Q.M., D.B., E.B., C.L., K.K.) designed the analysis and the methodology. C.B.S and Q.M. pre-processed and analysed the climate data. R.H. set up the statistical model and generated the figures. R.H., C.B.S., C.L. and K.K. analysed the results and wrote the manuscript. All authors (RH., C.B.S., Q.M., D.B., E.B., C.L., K.K.) reviewed and edited the manuscript.

Conflict of interest

'There are no competing interests to declare.

Data availability statement

All used data sets are described in the Methods Section.

- USDA dataset: `https://quickstats.nass.usda.gov/`, last access: 15 November 2022
- European crops: Ronchetti et al. (2024) (`https://doi.org/10.2905/685949ff-56de-4646-a8df-844b5bb5f835`)
- EUROSTAT dataset: `https://ec.europa.eu/eurostat/web/agriculture/`
- CPC Global Unified Temperature data provided by the NOAA PSL, Boulder, Colorado, USA, from their website at `https://psl.noaa.gov`
- Icons used in Fig. 1 are sourced from the noun project (`https://thenounproject.com`), downloaded on the pro-membership *carmenbeatriz.steinmann*. Image numbers include icons with Image number 4028435 (heat); 4546214 (soil moisture); 1179620, 1078364, 1673868, 1179616 (crops).

References

Aggarwal, P., Vyas, S., Thornton, P., Campbell, B. M. and Kropff, M. (2019). Importance of considering technology growth in impact assessments of climate change on agriculture, *Global Food Security* **23**: 41–48.

Antoniou, C., Savvides, A., Christou, A. and Fotopoulos, V. (2016). Unravelling chemical priming machinery in plants: the role of reactive oxygen–nitrogen–sulfur species in abiotic stress tolerance enhancement, *Current Opinion in Plant Biology* **33**: 101–107.
URL: *https://www.sciencedirect.com/science/article/pii/S1369526616301030*

Asseng, S., Ewert, F., Martre, P., Rötter, R. P., Lobell, D. B., Cammarano, D., Kimball, B. A., Ottman, M. J., Wall, G. W., White, J. W., Reynolds, M. P., Alderman, P. D., Prasad, P. V. V., Aggarwal, P. K., Anothai, J., Basso, B., Biernath, C., Challinor, A. J., De Sanctis, G., Doltra, J., Fereres, E., Garcia-Vila, M., Gayler, S., Hoogenboom, G., Hunt, L. A., Izaurralde, R. C., Jabloun, M., Jones, C. D., Kersebaum, K. C., Koehler, A.-K., Müller, C., Naresh Kumar, S., Nendel, C., O'Leary, G., Olesen, J. E., Palosuo, T., Priesack, E., Eyshi Rezaei, E., Ruane, A. C., Semenov, M. A., Shcherbak, I., Stöckle, C., Stratonovitch, P., Streck, T., Supit, I., Tao, F., Thorburn, P. J., Waha, K., Wang, E., Wallach, D., Wolf, J., Zhao, Z. and Zhu, Y. (2015). Rising temperatures reduce global wheat production, *Nature Climate Change* **5**(2): 143–147.
URL: *https://doi.org/10.1038/nclimate2470*

Baldwin, J. W., Dessy, J. B., Vecchi, G. A. and Oppenheimer, M. (2019). Temporally Compound Heat Wave Events and Global Warming: An Emerging Hazard, *Earth's Future* **7**(4): 411–427.
URL: *https://agupubs.onlinelibrary.wiley.com/doi/abs/10.1029/2018EF000989*

Ben-Ari, T., Boé, J., Ciais, P., Lecerf, R., Van der Velde, M. and Makowski, D. (2018). Causes and implications of the unforeseen 2016 extreme yield loss in the breadbasket of France, *Nature Communications* **9**(1): 1627.
URL: *https://www.nature.com/articles/s41467-018-04087-x*

Bessembinder, J., Bintanja, R., van Dorland, R., Homan, C., Overbeek, B., Selten, F. and Siegmund, P. (2023). KNMI'23 klimaatscenario's voor Nederland, *Technical report*.
URL: *https://cdn.knmi.nl/system/data*$_c$*enter*$_p$*ublications/files*/000/071/901/*original*/$KNMI23_k$*lima*
03.*pdf*

Butler, E. E. and Huybers, P. (2015). Variations in the sensitivity of US maize yield to extreme temperatures by region and growth phase, *Environmental Research Letters* **10**(3): 034009.
URL: *https://iopscience.iop.org/article/10.1088/1748-9326/10/3/034009*

Butler, T. J., Celen, A. E., Webb, S. L., Krstic, D. and Interrante, S. M. (2014). Temperature Affects the Germination of Forage Legume Seeds, *Crop Science* **54**(6): 2846–2853.
URL: *https://doi.org/10.2135/cropsci2014.01.0063*

Cheng, S., Huang, J., Ji, F. and Lin, L. (2017). Uncertainties of soil moisture in historical simulations and future projections, *Journal of Geophysical Research: Atmospheres* **122**(4): 2239–2253.
URL: *https://doi.org/10.1002/2016JD025871*

Choudhury, F. K., Rivero, R. M., Blumwald, E. and Mittler, R. (2017). Reactive oxygen species, abiotic stress and stress combination, *The Plant Journal* **90**(5): 856–867.
URL: *https://doi.org/10.1111/tpj.13299*

Dixit, S., Sivalingam, P. N., Baskaran, R. K. M., Senthil-Kumar, M. and Ghosh, P. K. (2024). Plant responses to concurrent abiotic and biotic stress: unravelling physiological and morphological mechanisms, *Plant Physiology Reports* **29**(1): 6–17.

Dong, J., Lei, F. and Crow, W. T. (2022). Land transpiration-evaporation partitioning errors responsible for modeled summertime warm bias in the central United States, *Nature Communications* **13**(1): 336.
URL: *https://doi.org/10.1038/s41467-021-27938-6*

Gloege, L., Kornhuber, K., Skulovich, O., Pal, I., Zhou, S., Ciais, P. and Gentine, P. (2022). Land-Atmosphere Cascade Fueled the 2020 Siberian Heatwave, *AGU Advances* **3**(6): e2021AV000619.
URL: *https://doi.org/10.1029/2021AV000619*

Hamed, R., Lesk, C., Shepherd, T. G., Goulart, H. M. D., van Garderen, L., van den Hurk, B. and Coumou, D. (2025). One-third of the global soybean production failure in 2012 is attributable to climate change, *Communications Earth & Environment* **6**(1): 199.
URL: *https://doi.org/10.1038/s43247-025-02171-x*

Hamed, R., Van Loon, A., Aerts, J. and Coumou, D. (2021). Impacts of compound hot–dry extremes on US soybean yields, *Earth System Dynamics* **12**: 1371–1391.

Heinicke, S., Frieler, K., Jägermeyr, J. and Mengel, M. (2022). Global gridded crop models underestimate yield responses to droughts and heatwaves, *Environmental Research Letters* **17**(4): 044026.
URL: *https://iopscience.iop.org/article/10.1088/1748-9326/ac592e*

Hossain, M. A., Li, Z.-G., Hoque, T. S., Burritt, D. J., Fujita, M. and Munné-Bosch, S. (2018). Heat or cold priming-induced cross-tolerance to abiotic stresses in plants: key regulators and possible mechanisms, *Protoplasma* **255**(1): 399–412.
URL: *https://doi.org/10.1007/s00709-017-1150-8*

Hu, Q., Weiss, A., Feng, S. and Baenziger, P. S. (2005). Earlier winter wheat heading dates and warmer spring in the U.S. Great Plains, *Agricultural and Forest Meteorology* **135**(1-4): 284–290.

Jacott, C. N. and Boden, S. A. (2020). Feeling the heat: developmental and molecular responses of wheat and barley to high ambient temperatures, *Journal of Experimental Botany* **71**(19): 5740–5751.
URL: *https://doi.org/10.1093/jxb/eraa326*

Jagadish, S. V. K., Way, D. A. and Sharkey, T. D. (2021). Plant heat stress: Concepts directing future research, *Plant, Cell & Environment* **44**(7): 1992–2005.
URL: *https://doi.org/10.1111/pce.14050*

Kebede, E. A., Oluoch, K. O., Siebert, S., Mehta, P., Hartman, S., Jägermeyr, J., Ray, D., Ali, T., Brauman, K. A., Deng, Q., Xie, W. and Davis, K. F. (2025). A global open-source dataset of monthly irrigated and rainfed cropped areas (MIRCA-OS) for the 21st century, *Scientific Data* **12**(1): 208.
URL: *https://doi.org/10.1038/s41597-024-04313-w*

Kornhuber, K., Lesk, C., Schleussner, C. F., Jägermeyr, J., Pfleiderer, P. and Horton, R. M. (2023). Risks of synchronized low yields are underestimated in climate and crop model projections, *Nature Communications* **14**(1): 3528.
URL: *https://doi.org/10.1038/s41467-023-38906-7*

Lesk, C., Anderson, W., Rigden, A., Coast, O., Jägermeyr, J., McDermid, S., Davis, K. F. and Konar, M. (2022). Compound heat and moisture extreme impacts on global crop yields under climate change, *Nature Reviews Earth & Environment* **3**(12): 872–889.
URL: *https://doi.org/10.1038/s43017-022-00368-8*

Lesk, C., Coffel, E., Winter, J., Ray, D., Zscheischler, J., Seneviratne, S. I. and Horton, R. (2021). Stronger temperature–moisture couplings exacerbate the impact of climate warming on global crop yields, *Nature Food* **2**(9): 683–691.
URL: *https://doi.org/10.1038/s43016-021-00341-6*

Lesk, C., Rowhani, P. and Ramankutty, N. (2016). Influence of extreme weather disasters on global crop production, *Nature* **529**(7584): 84–87.
URL: *https://www.nature.com/articles/nature16467*

Liu, B., Asseng, S., Müller, C., Ewert, F., Elliott, J., Lobell, D., Martre, P., Ruane, A., Wallach, D., Jones, J., Rosenzweig, C., Aggarwal, P., Alderman, P., Anothai, J., Basso, B., Biernath, C., Cammarano, D., Challinor, A., Deryng, D., Sanctis, G., Doltra, J., Fereres, E., Folberth, C., Garcia-Vila, M., Gayler, S., Hoogenboom, G., Hunt, L., Izaurralde, R., Jabloun, M., Jones, C., Kersebaum, K., Kimball, B., Koehler, A.-K., Kumar, S., Nendel, C., O'Leary, G., Olesen, J., Ottman, M., Palosuo, T., Prasad, P., Priesack, E., Pugh, T., Reynolds, M., Rezaei, E., Rötter, R., Schmid, E., Semenov, M., Shcherbak, I., Stehfest, E., Stöckle, C., Stratonovitch, P., Streck, T., Supit, I., Tao, F., Thorburn, P., Waha, K., Wall, G., Wang, E., White, J., Wolf, J., Zhao, Z. and Zhu, Y. (2016). Similar estimates of temperature impacts on global wheat yield by three independent methods, *Nature Climate Change* **6**(12): 1130–1136.

Liu, H., Able, A. J. and Able, J. A. (2022). Priming crops for the future: rewiring stress memory, *Trends in Plant Science* **27**(7): 699–716.
URL: *https://www.sciencedirect.com/science/article/pii/S1360138521003216*

Martens, B., Miralles, D. G., Lievens, H., van der Schalie, R., de Jeu, R. A. M., Fernández-Prieto, D., Beck, H. E., Dorigo, W. A. and Verhoest, N. E. C. (2017). GLEAM v3: satellite-based land evaporation and root-zone soil moisture, *Geoscientific Model Development* **10**(5): 1903–1925.
URL: *https://gmd.copernicus.org/articles/10/1903/2017/*

Mendanha, T., Rosenqvist, E., Hyldgaard, B. and Ottosen, C.-O. (2018). Heat priming effects on anthesis heat stress in wheat cultivars (Triticum aestivum L.) with contrasting tolerance to heat stress, *Plant Physiology and Biochemistry* **132**: 213–221.
URL: *https://www.sciencedirect.com/science/article/pii/S0981942818304005*

Miralles, D. G., Teuling, A. J., van Heerwaarden, C. C. and Vilà-Guerau de Arellano, J. (2014). Mega-heatwave temperatures due to combined soil desiccation and atmospheric heat accumulation, *Nature Geoscience* **7**(5): 345–349.
URL: *https://doi.org/10.1038/ngeo2141*

Mittler, R., Finka, A. and Goloubinoff, P. (2012). How do plants feel the heat?, *Trends in Biochemical Sciences* **37**(3): 118–125.
URL: *https://www.sciencedirect.com/science/article/pii/S0968000411002015*

Nadeem, M., Li, J., Wang, M., Shah, L., Lu, S., Wang, X. and Ma, C. (2018). Unraveling Field Crops Sensitivity to Heat Stress: Mechanisms, Approaches, and Future Prospects, *Agronomy* **8**(7).
URL: *https://www.mdpi.com/2073-4395/8/7/128*

Nóia Júnior, R. d. S., Asseng, S., Müller, C., Deswarte, J.-C., Cohan, J.-P. and Martre, P. (2025). Negative impacts of climate change on crop yields are underestimated, *Trends in Plant Science* .
URL: *https://doi.org/10.1016/j.tplants.2025.05.002*

Ortiz-Bobea, A., Wang, H., Carrillo, C. M. and Ault, T. R. (2019). Unpacking the climatic drivers of US agricultural yields, *Environmental Research Letters*

14(6): 064003.
URL: *https://iopscience.iop.org/article/10.1088/1748-9326/ab1e75*

Proctor, J., Rigden, A., Chan, D. and Huybers, P. (2022). More accurate specification of water supply shows its importance for global crop production, *Nature Food* **3**(9): 753–763.
URL: *https://doi.org/10.1038/s43016-022-00592-x*

Ray, D. K., West, P. C., Clark, M., Gerber, J. S., Prishchepov, A. V. and Chatterjee, S. (2019). Climate change has likely already affected global food production, *PLOS ONE* **14**(5): e0217148.
URL: *https://dx.plos.org/10.1371/journal.pone.0217148*

Raymond, C., Suarez-Gutierrez, L., Kornhuber, K., Pascolini-Campbell, M., Sillmann, J. and Waliser, D. E. (2022). Increasing spatiotemporal proximity of heat and precipitation extremes in a warming world quantified by a large model ensemble, *Environmental Research Letters* **17**(3): 035005.
URL: *https://iopscience.iop.org/article/10.1088/1748-9326/ac5712*

Ren, S., Qin, Q. and Ren, H. (2019). Contrasting wheat phenological responses to climate change in global scale, *Science of The Total Environment* **665**: 620–631.

Rezaei, E. E., Siebert, S. and Ewert, F. (2015). Intensity of heat stress in winter wheat—phenology compensates for the adverse effect of global warming, *Environmental Research Letters* **10**(2): 024012.
URL: *https://iopscience.iop.org/article/10.1088/1748-9326/10/2/024012*

Rigden, A. J., Mueller, N. D., Holbrook, N. M., Pillai, N. and Huybers, P. (2020). Combined influence of soil moisture and atmospheric evaporative demand is important for accurately predicting US maize yields, *Nature Food* **1**(2): 127–133.
URL: *https://doi.org/10.1038/s43016-020-0028-7*

Robinson, A., Lehmann, J., Barriopedro, D., Rahmstorf, S. and Coumou, D. (2021). Increasing heat and rainfall extremes now far outside the historical climate, *npj Climate and Atmospheric Science* **4**(1): 45.
URL: *https://doi.org/10.1038/s41612-021-00202-w*

Ronchetti, G., Nisini Scacchiafichi, L., Seguini, L., Cerrani, I. and van der Velde, M. (2024). Harmonized European Union subnational crop statistics can reveal climate impacts and crop cultivation shifts, *Earth System Science Data* **16**(3): 1623–1649.
URL: *https://essd.copernicus.org/articles/16/1623/2024/*

Sacks, W. J., Deryng, D., Foley, J. A. and Ramankutty, N. (2010). Crop planting dates: an analysis of global patterns, *Global Ecology and Biogeography* pp. no–no.
URL: *https://onlinelibrary.wiley.com/doi/10.1111/j.1466-8238.2010.00551.x*

Schewe, J., Gosling, S. N., Reyer, C., Zhao, F., Ciais, P., Elliott, J., Francois, L., Huber, V., Lotze, H. K., Seneviratne, S. I., van Vliet, M. T. H., Vautard, R., Wada, Y., Breuer, L., Büchner, M., Carozza, D. A., Chang, J., Coll, M., Deryng, D., de Wit, A., Eddy, T. D., Folberth, C., Frieler, K., Friend, A. D., Gerten, D., Gudmundsson,

L., Hanasaki, N., Ito, A., Khabarov, N., Kim, H., Lawrence, P., Morfopoulos, C., Müller, C., Müller Schmied, H., Orth, R., Ostberg, S., Pokhrel, Y., Pugh, T. A. M., Sakurai, G., Satoh, Y., Schmid, E., Stacke, T., Steenbeek, J., Steinkamp, J., Tang, Q., Tian, H., Tittensor, D. P., Volkholz, J., Wang, X. and Warszawski, L. (2019). State-of-the-art global models underestimate impacts from climate extremes, *Nature Communications* **10**(1): 1005.
URL: *https://doi.org/10.1038/s41467-019-08745-6*

Shepherd, T. G. (2014). Atmospheric circulation as a source of uncertainty in climate change projections, *Nature Geoscience* **7**(10): 703–708.
URL: *https://doi.org/10.1038/ngeo2253*

Sippel, S., Zscheischler, J., Mahecha, M. D., Orth, R., Reichstein, M., Vogel, M. and Seneviratne, S. I. (2017). Refining multi-model projections of temperature extremes by evaluation against land–atmosphere coupling diagnostics, *Earth System Dynamics* **8**(2): 387–403.
URL: *https://esd.copernicus.org/articles/8/387/2017/*

Stagge, J. H., Tallaksen, L. M., Gudmundsson, L., Van Loon, A. F. and Stahl, K. (2015). Candidate Distributions for Climatological Drought Indices (SPI and SPEI), *International Journal of Climatology* **35**(13): 4027–4040.
URL: *https://doi.org/10.1002/joc.4267*

Suzuki, N., Rivero, R. M., Shulaev, V., Blumwald, E. and Mittler, R. (2014). Abiotic and biotic stress combinations, *New Phytologist* **203**(1): 32–43.
URL: *https://doi.org/10.1111/nph.12797*

Troy, T. J., Kipgen, C. and Pal, I. (2015). The impact of climate extremes and irrigation on US crop yields, *Environmental Research Letters* **10**(5): 054013.

Vogel, J., Rivoire, P., Deidda, C., Rahimi, L., Sauter, C. A., Tschumi, E., van der Wiel, K., Zhang, T. and Zscheischler, J. (2021). Identifying meteorological drivers of extreme impacts: an application to simulated crop yields, *Earth System Dynamics* **12**(1): 151–172.
URL: *https://esd.copernicus.org/articles/12/151/2021/*

WANG, X., LIU, F.-l. and JIANG, D. (2017). Priming: A promising strategy for crop production in response to future climate, *Journal of Integrative Agriculture* **16**(12): 2709–2716.
URL: *https://www.sciencedirect.com/science/article/pii/S2095311917617866*

Weiland, R. S., van der Wiel, K., Selten, F. and Coumou, D. (2021). Intransitive Atmosphere Dynamics Leading to Persistent Hot–Dry or Cold–Wet European Summers, *Journal of Climate* **34**(15): 6303–6317.
URL: *https://journals.ametsoc.org/view/journals/clim/34/15/JCLI-D-20-0943.1.xml*

Zscheischler, J., Westra, S., {van den Hurk}, B. J. J. M., Seneviratne, S. I., Ward, P. J., Pitman, A., AghaKouchak, A., Bresch, D. N., Leonard, M., Wahl, T. and Zhang, X.

(2018). Future climate risk from compound events, *Nature Climate Change* **8**(6): 469–
477.
URL: *http://www.nature.com/articles/s41558-018-0156-3*

Submitted to: *Environ. Res. Lett.*

Supplementary Information: Amplified agricultural impacts from more frequent and intense sequential heat events

Raed Hamed[1*], Carmen B. Steinmann[2,3*], Qiyun Ma[4], Daniel Balanzategui[5,6,7], Ellie Broadman[8], Corey Lesk[9] and Kai Kornhuber[10,11]

[1]Institute for Environmental Studies (IVM), Vrije Universiteit Amsterdam, Amsterdam, 1081, the Netherlands.
[2]Institute for Environmental Decisions, ETH Zurich, Zurich, 8092, Switzerland.
[3] Federal Office of Meteorology and Climatology MeteoSwiss, Zurich, 8058, Switzerland
[4] Alfred Wegener Institute, Helmholtz Centre for Polar and Marine Research, Bremerhaven, 27570, Germany.
[5] Materials Testing Institute, University of Applied Sciences, Luebeck, 23562, Germany.
[6] Department of Natural Sciences, German Archaeology Institute DAI, Berlin, 14195, Germany.
[7] Geography Department, Humboldt University of Berlin, Berlin, 10117, Germany.
[8] Laboratory of Tree-Ring Research, University of Arizona, Tucson, 85721, USA.
[9] Department of Geography, Neukom Institute for Computational Science, Dartmouth College, Hanover, 03755, USA.
[10] Lamont-Doherty Earth Observatory, Columbia University, Palisades, 10964, USA.
[11] International Institute for Applied Systems Analysis, Laxenburg, 2361, Austria.
*These authors contributed equally to this work.

E-mail: carmen.steinmann@usys.ethz.ch

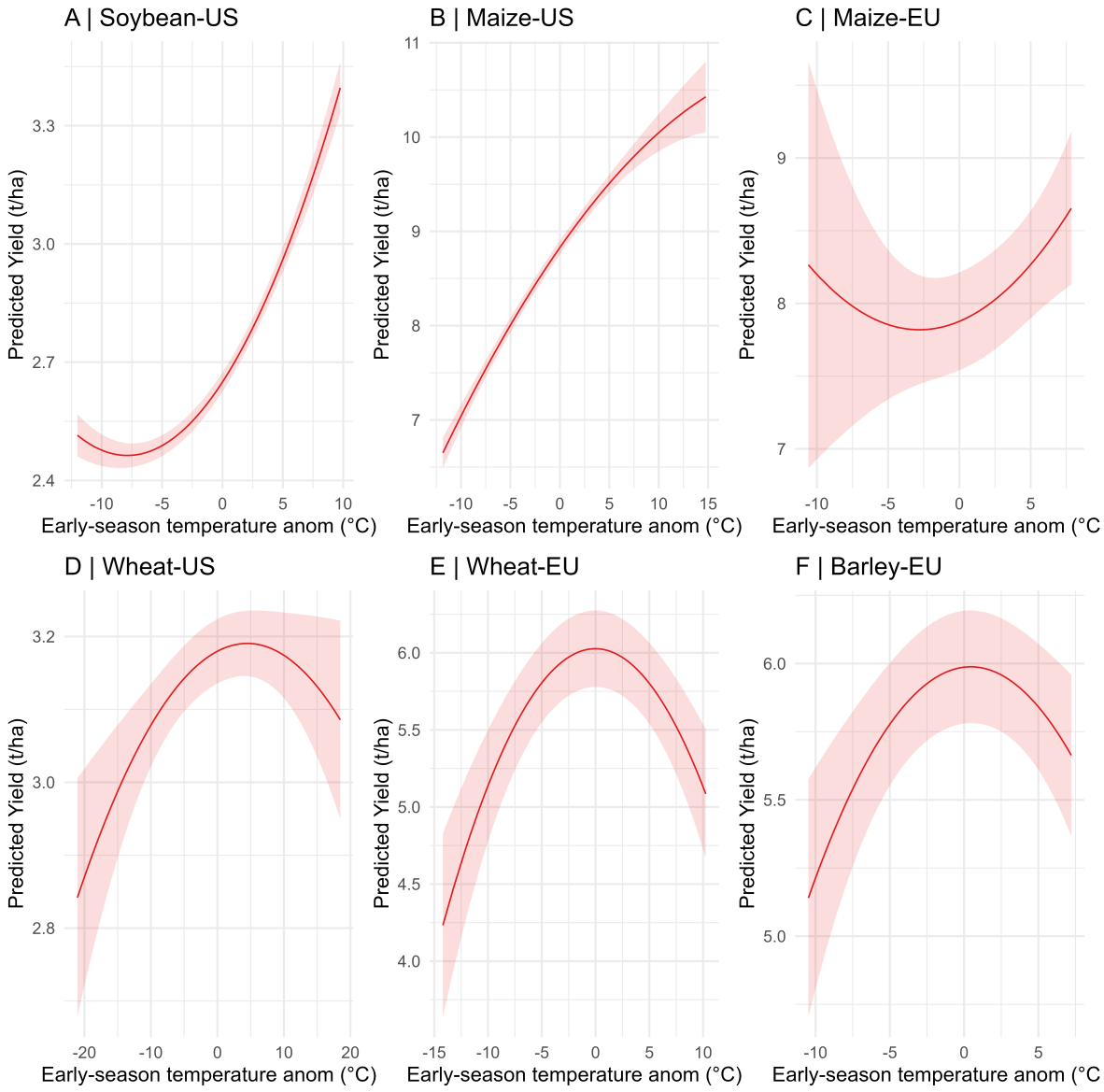

Figure S1. Marginal effect of early-season temperature anomalies on crop yield. Values represent changes in yield (t/ha) per °C anomaly in early-season mean maximum temperature

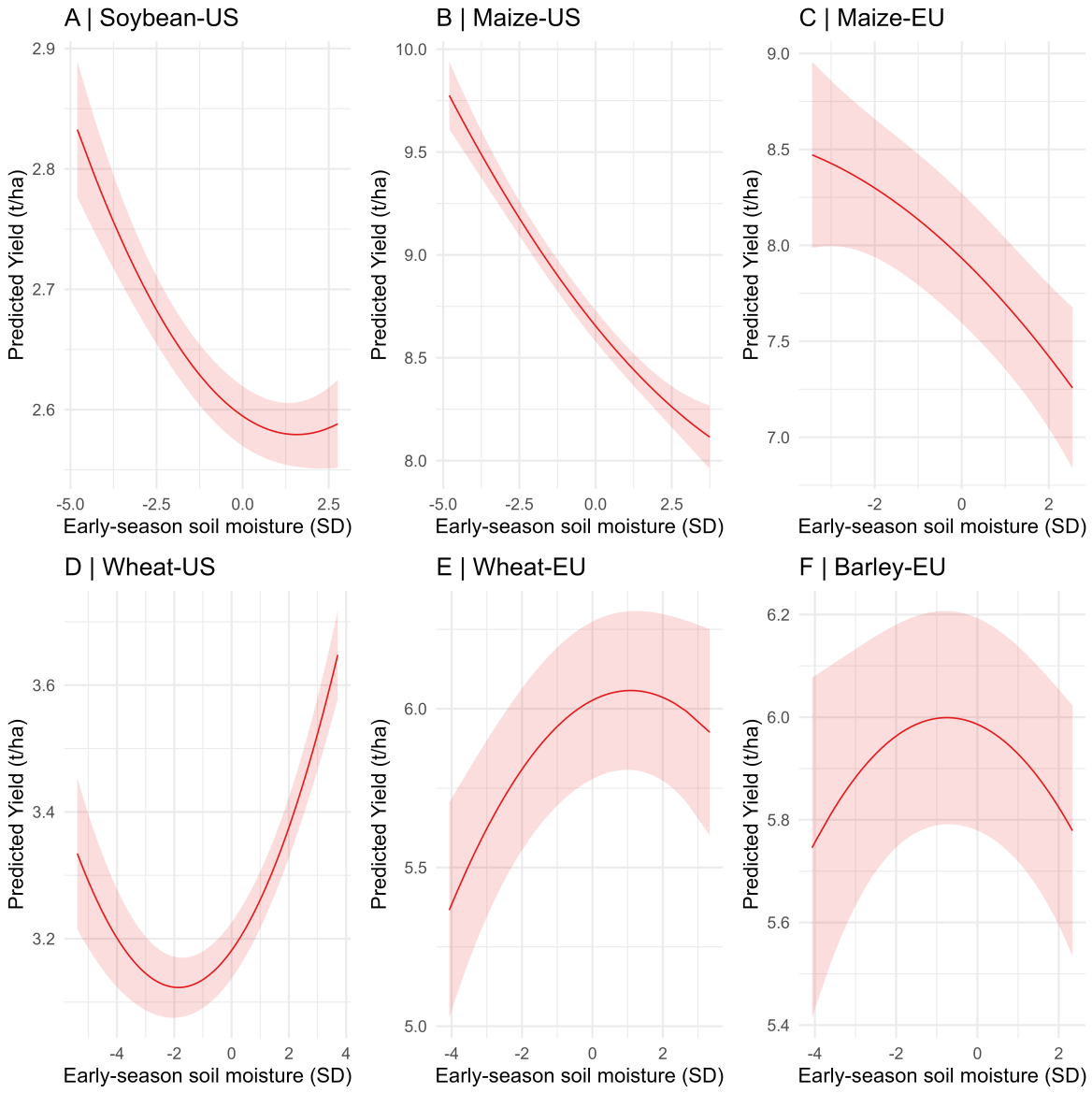

Figure S2. Marginal effect of early-season soil moisture anomalies on crop yield. Values represent changes in yield (t/ha) per standard deviation anomaly in early-season mean soil moisture

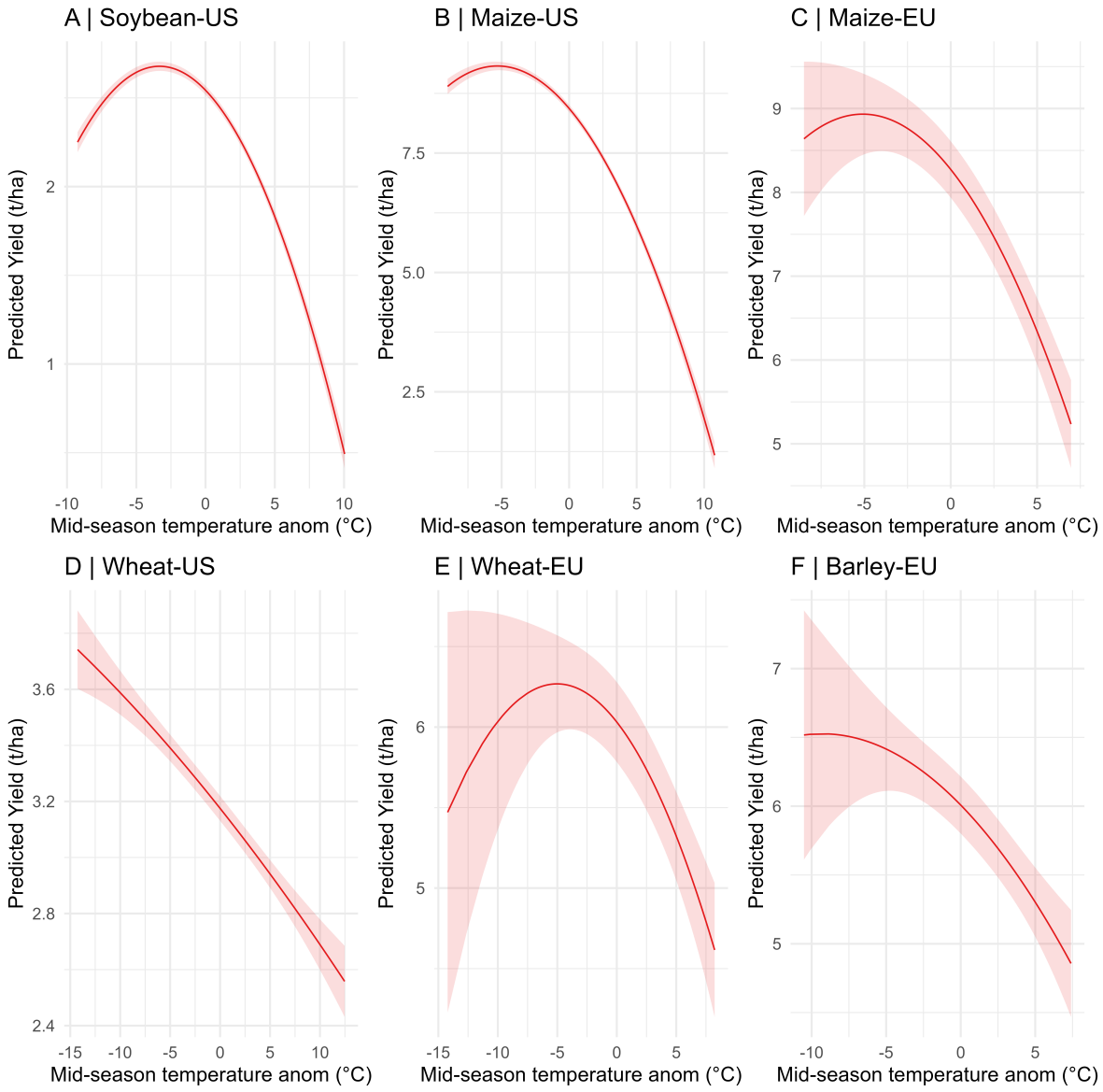

Figure S3. Marginal effect of mid-season temperature anomalies on crop yield. Values represent changes in yield (t/ha) per °C anomaly in mid-season mean maximum temperature

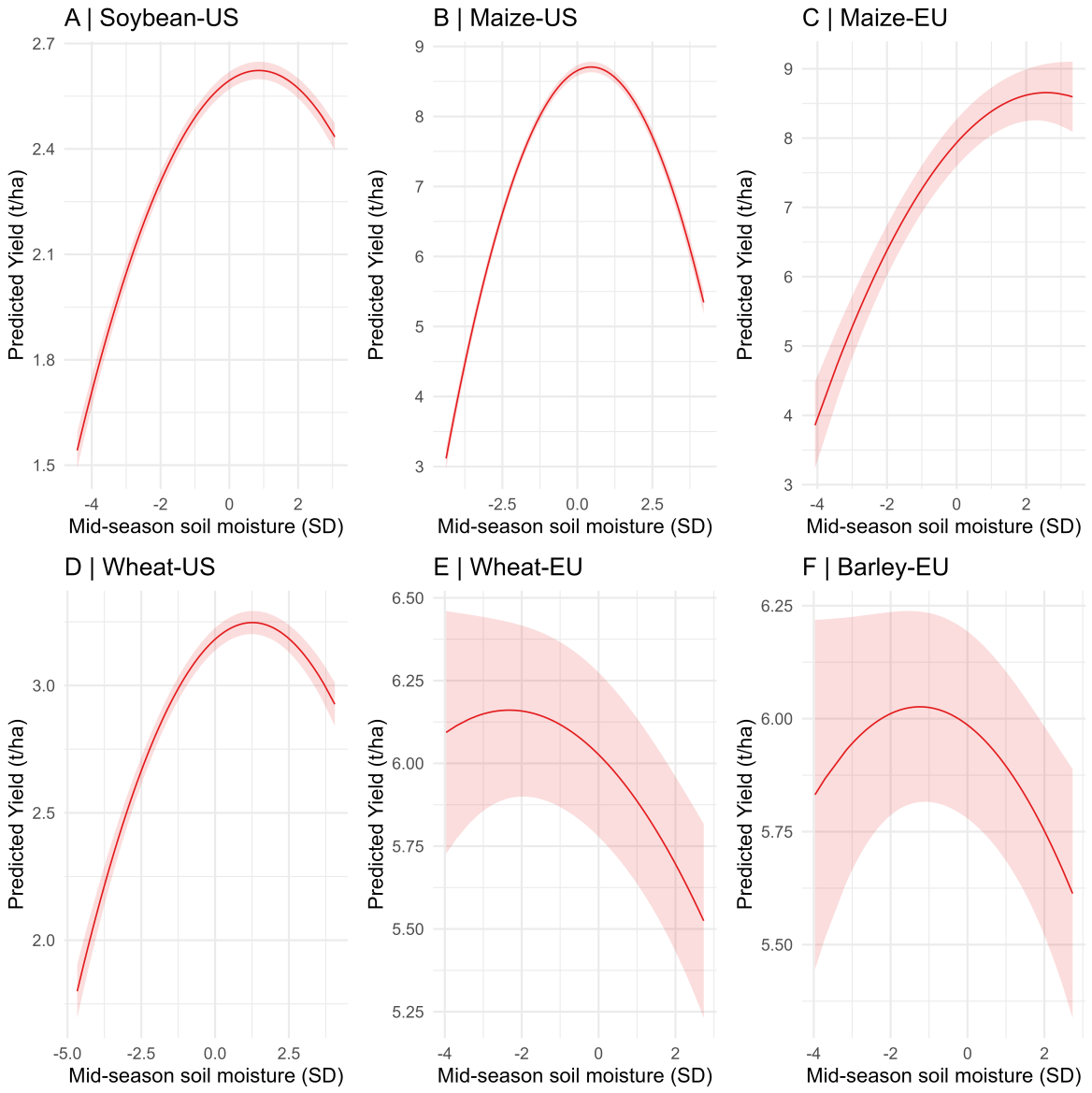

Figure S4. Marginal effect of mid-season soil moisture anomalies on crop yield. Values represent changes in yield (t/ha) per standard deviation anomaly in mid-season mean soil moisture

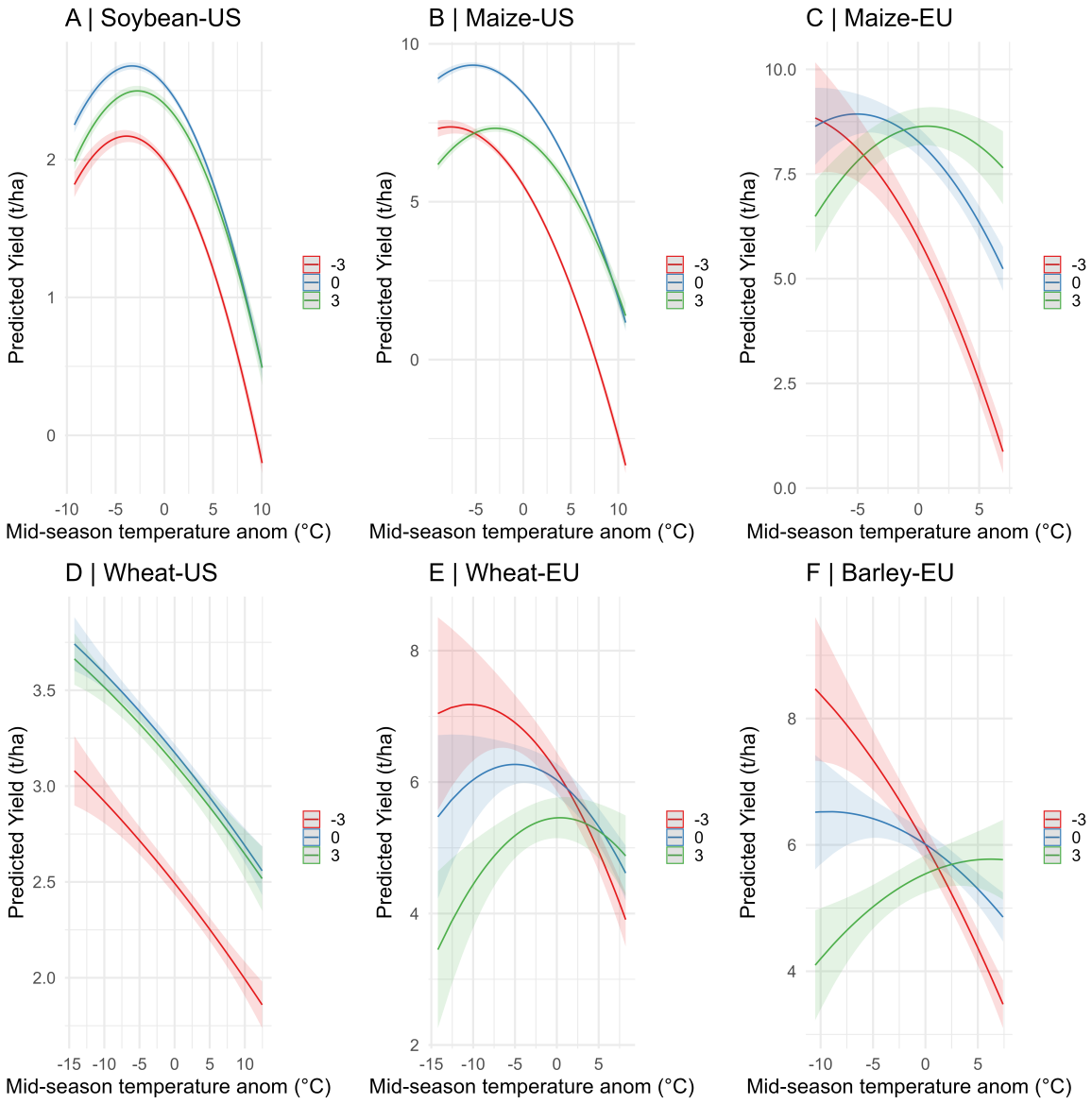

Figure S5. Marginal effect of mid-season temperature anomalies on crop yield, conditional on soil moisture levels. Values represent changes in yield (t/ha) per °C anomaly in mid-season mean maximum temperature, evaluated at three mid-season soil moisture anomaly levels: -3 (dry), 0 (normal), and +3 (wet). Soil moisture anomalies are expressed in units of standard deviation

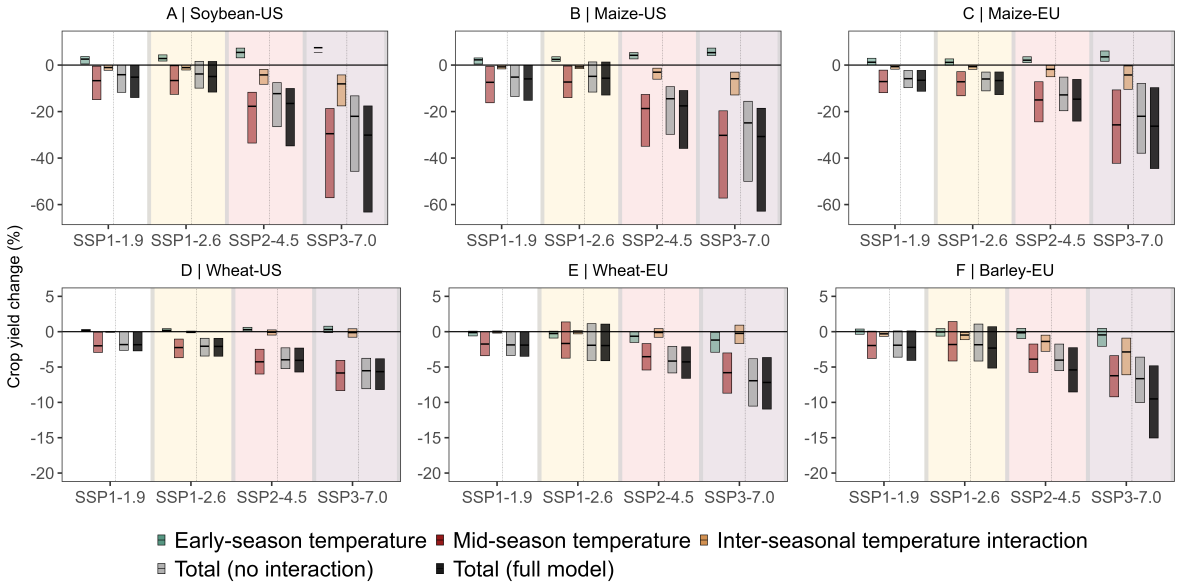

Figure S6. Projected crop production changes for the future period (2060–2100) compared to historic (1975–2015) under different emission scenarios for a subset of 8 climate models shared across SSPs. SSP1-1.9 (number models n=8), SSP1-2.6 (n=8), SSP2-4.5 (n=8), SSP3-7.0(n=8). Average crop yield losses are attributed to early- and mid-season temperature changes and their interaction. Bar show average projected losses, while error bars show the 5–95% range accounting for regression and model projection uncertainties.

Table S 1. Regression results by crop and region (Part 1: A–C)

	A — Soybean-US		B — Maize-US		C — Maize-EU	
Predictors	Estimates	CI	Estimates	CI	Estimates	CI
(Intercept)	2.58 ***	2.55 – 2.60	8.52 ***	8.44 – 8.59	8.11 ***	7.77 – 8.44
early-season T	0.04 ***	0.04 – 0.04	0.13 ***	0.13 – 0.14	0.06 ***	0.03 – 0.09
mid-season T	-0.10 ***	-0.10 – -0.09	-0.36 ***	-0.37 – -0.35	-0.24 ***	-0.28 – -0.20
early-season M	-0.02 ***	-0.02 – -0.01	-0.18 ***	-0.20 – -0.17	-0.22 ***	-0.27 – -0.17
mid-season M	0.07 ***	0.06 – 0.07	0.26 ***	0.24 – 0.27	0.44 ***	0.39 – 0.50
early-season T^2	0.00 ***	0.00 – 0.00	-0.00 ***	-0.00 – -0.00	0.01	-0.00 – 0.02
mid-season T^2	-0.01 ***	-0.01 – -0.01	-0.03 ***	-0.03 – -0.03	-0.03 ***	-0.04 – -0.02
early-season M^2	0.01 ***	0.00 – 0.01	0.01 **	0.00 – 0.02	-0.02	-0.05 – 0.01
mid-season M^2	-0.04 ***	-0.04 – -0.04	-0.24 ***	-0.25 – -0.23	-0.11 ***	-0.14 – -0.08
year	0.03 ***	0.03 – 0.03	0.12 ***	0.12 – 0.12	0.09 ***	0.08 – 0.11
early-season T × mid-season T	-0.01 ***	-0.01 – -0.01	-0.03 ***	-0.03 – -0.02	-0.02 *	-0.03 – -0.00
mid-season T × mid-season M	0.00 ***	0.00 – 0.01	0.05 ***	0.04 – 0.05	0.10 ***	0.08 – 0.12
Counties	1191		1470		66	
Observations	46561		56997		2039	

* $p < 0.05$ ** $p < 0.01$ *** $p < 0.001$

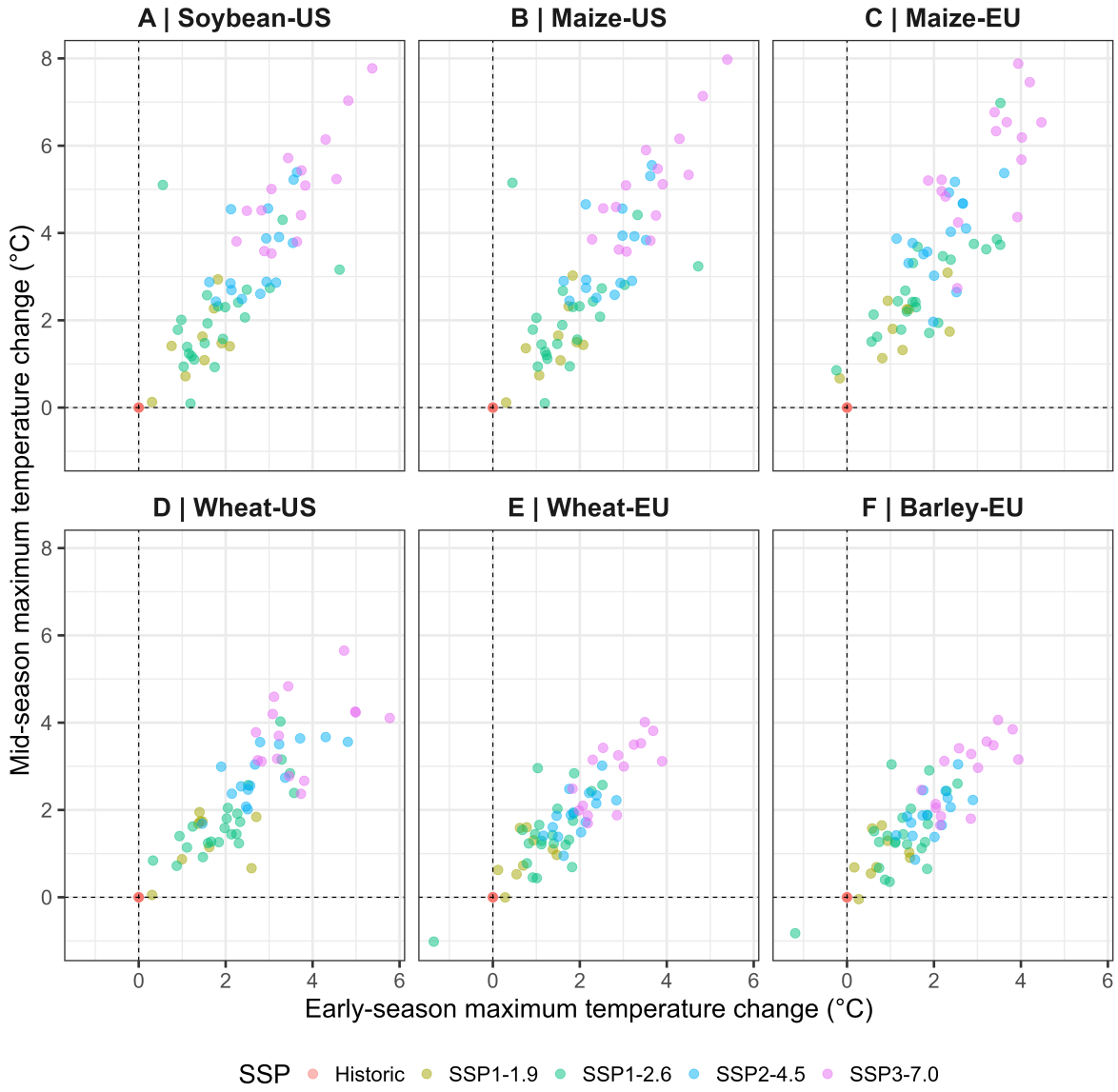

Figure S7. Projected changes in early- and mid-season temperature conditions. Changes are displayed across models and SSPs, relative to each model's historical baseline. Each point represents the mean seasonal temperature anomaly (°C) for a given model and scenario, with anomalies calculated relative to that model's own historical period.

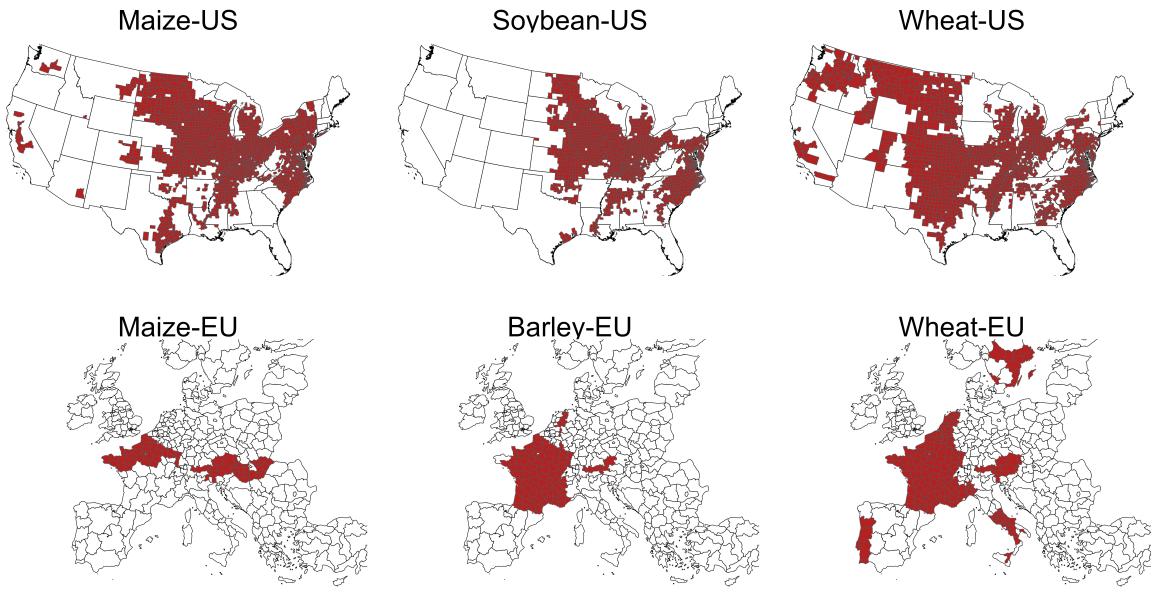

Figure S8. Counties included in the analysis. Counties shown in red meet all selection criteria: over 90% rainfed area, at least 25 years of yield and weather data, and crop calendars consistent with defined early- and mid-season periods—April–May and July–August for soybean and maize, and January–February and April-May for wheat and barley.

Table S 2. Regression results by crop and region (Part 2: D–F)

	D — Wheat-US		E — Wheat-EU		F — Barley-EU	
Predictors	Estimates	CI	Estimates	CI	Estimates	CI
(Intercept)	3.14 ***	3.09 – 3.18	6.04 ***	5.79 – 6.29	6.01 ***	5.80 – 6.22
early-season T	0.00 ***	0.00 – 0.01	-0.00	-0.01 – 0.01	0.01	-0.00 – 0.02
mid-season T	-0.04 ***	-0.05 – -0.04	-0.09 ***	-0.11 – -0.08	-0.11 ***	-0.13 – -0.09
early-season M	0.06 ***	0.06 – 0.07	0.06 ***	0.03 – 0.08	-0.03 *	-0.07 – -0.00
mid-season M	0.10 ***	0.10 – 0.11	-0.12 ***	-0.15 – -0.09	-0.08 ***	-0.11 – -0.05
early-season T^2	-0.00 **	-0.00 – -0.00	-0.01 ***	-0.01 – -0.01	-0.01 ***	-0.01 – -0.00
mid-season T^2	-0.00	-0.00 – 0.00	-0.01 ***	-0.01 – -0.00	-0.01	-0.01 – 0.00
early-season M^2	0.02 ***	0.01 – 0.02	-0.03 ***	-0.04 – -0.01	-0.02 **	-0.04 – -0.01
mid-season M^2	-0.04 ***	-0.05 – -0.04	-0.02 **	-0.04 – -0.01	-0.03 *	-0.05 – -0.00
year	0.03 ***	0.03 – 0.03	0.03 ***	0.02 – 0.03	0.03 ***	0.02 – 0.03
early-season T × mid-season T	-0.00	-0.00 – 0.00	-0.00	-0.01 – 0.00	-0.02 ***	-0.03 – -0.01
mid-season T × mid-season M	0.00	-0.00 – 0.00	0.03 ***	0.02 – 0.04	0.06 ***	0.05 – 0.08
Counties	1447		176		99	
Observations	51529		5310		3178	

* $p < 0.05$ ** $p < 0.01$ *** $p < 0.001$

Table S 3. CMIP6 models considered per SSP scenario

	1-1.9	1-2.6	2-4.5	3-7.0
ACCESS-CM2		X	X	X
ACCESS-ESM1-5		X		
AWI-CM-1-1-MR		X	X	X
BCC-CSM2-MR		X	X	X
CANESM5	X	X	X	X
CISESM		X		
CMCC-ESM2		X		
EC-EARTH3		X	X	X
EC-EARTH3-Veg	X	X	X	X
EC-EARTH3-Veg-LR	X	X		
FGOALS-g3	X	X	X	X
FIO-ESM-2-0		X		
GFDL-ESM4	X	X	X	X
INM-CM4-8		X	X	X
INM-CM5-0		X	X	X
IPSL-CM6A-LR	X	X	X	X
KACE-1-0-G		X		
MIROC6	X	X	X	X
MPI-ESM1-2-HAM				
MPI-ESM1-2-HR		X	X	X
MPI-ESM1-2-LR	X	X	X	X
MRI-ESM2-0	X	X	X	X
NESM3		X		
Number of models	9	22	15	15